The solvent shell structure of aqueous iodide: X-ray absorption spectroscopy and classical, hybrid QM/MM and full quantum molecular dynamics simulations

ARTICLE *in* CHEMICAL PHYSICS · FEBRUARY 2010

Impact Factor: 1.65 · DOI: 10.1016/j.chemphys.2010.03.023 · Source: OAI

7 AUTHORS, INCLUDING:

Van-Thai Pham
Vietnam Academy of Science and Technology
43 PUBLICATIONS **953** CITATIONS
SEE PROFILE

Ivano Tavernelli
IBM
141 PUBLICATIONS **4,339** CITATIONS
SEE PROFILE

Chris Milne
Paul Scherrer Institut
97 PUBLICATIONS **1,419** CITATIONS
SEE PROFILE

Renske van der Veen
University of Illinois, Urbana-Champaign
35 PUBLICATIONS **676** CITATIONS
SEE PROFILE

Chemical Physics 371 (2010) 24–29

Contents lists available at ScienceDirect

Chemical Physics

journal homepage: www.elsevier.com/locate/chemphys

The solvent shell structure of aqueous iodide: X-ray absorption spectroscopy and classical, hybrid QM/MM and full quantum molecular dynamics simulations

V.T. Pham [a], I. Tavernelli [b], C.J. Milne [a], R.M. van der Veen [a], P. D'Angelo [c], Ch. Bressler [a], M. Chergui [a,*]

[a] Ecole Polytechnique Fédérale de Lausanne, Laboratoire de spectroscopie ultrarapide, ISIC, FSB-BSP, CH-1015 Lausanne, Switzerland
[b] Ecole Polytechnique Fédérale de Lausanne, Laboratoire de chimie et biochimie computationnelles, ISIC, FSB-BSP, CH-1015 Lausanne, Switzerland
[c] Dipartimento di Chimica, Università di Roma "La Sapienza", Ple A. Moro 5, 00185 Roma, Italy

ARTICLE INFO

Article history:
Received 22 December 2009
In final form 19 March 2010
Available online 24 March 2010

Keywords:
Aqueous halides
Solvation shell
X-ray absorption spectroscopy
EXAFS
Molecular dynamics
DFT
QM/MM

ABSTRACT

The L_3 X-ray absorption spectrum of aqueous iodide is reported, and its EXAFS is compared to theoretical spectra reconstructed from the radial distribution function of the iodide hydration obtained from classical, hybrid Quantum Mechanics Molecular Mechanics, (QM/MM) and full quantum (density functional theory, DFT) molecular dynamics simulations. Since EXAFS is mainly sensitive to short distances around the iodide ion, it is a direct probe of the local solvation structure. The comparison shows that QM/MM simulations deliver a satisfactory description of the EXAFS signal, while nonpolarizable classical simulations are somewhat less satisfactory and DFT-based simulations perform poorly. We also identify a weak anisotropy of the water solvation shell around iodide, which may be of importance in electron photoejection experiments.

1. Introduction

The properties of solvated ions and the role of the surrounding water molecules are important in a large variety of chemical reactions and biochemical processes [1,2]. They are also key for transport of ionic solutes in water [3], and ionic hydration dynamics play a central role in several physiological processes such as ion transport through membranes, where the hydration shell reorganizes in the initial and final stages of the membrane-crossing mechanism [4]. Despite the importance of this subject, the structure of the solvation shell and its dynamical behaviour are still intensely debated.

Various experimental and theoretical studies have been carried out on halides in water aimed at obtaining a complete description of the solvent shell structure and dynamics. X-ray and neutron diffraction studies yield coordination numbers that are significantly scattered, varying by almost a factor of two for nearly all halides [5,6]. In the case of iodide, which is the system of interest here, the first peak of the I–O radial distribution function (RdF) was found to be in the range of 3.55–3.76 Å, and the coordination numbers with oxygen atoms varied from 4 to 9. This spread of values underlines the difficulty of defining a solvation shell due to its diffuse character. To determine more precisely the solvent shell structure, hard X-ray absorption spectroscopy on the halides seems more appropriate, since by X-ray absorption near edge structure (XANES) and extended X-ray absorption fine structure (EXAFS) one probes the local structure around the atom of interest.

Tanida et al. [7] recorded L_1- and L_3-edge XANES spectra of aqueous I^- and compared them to simulated spectra assuming model geometries of clusters of water molecules around the ion. The spectra were satisfactorily described by taking into account the first hydration shell only. A somewhat similar approach was adopted by Merkling et al. [8] for both the XANES and the EXAFS of the bromide ion. They derived optimized geometries of $[Br(H_2O)_n]^-$ $(1 \leqslant n \leqslant 8)$ from quantum chemical calculations, and in order to reproduce the XANES spectra in a satisfactory way, they introduced statistical fluctuations, which in their case were obtained from snapshots of Monte Carlo (MC) simulations. The latter improvement underlines the complexity of the problem, which is already implicit from the above mentioned spread of coordination numbers and distances. In limiting their analysis to the first shell and to optimized geometries, the simulations of Tanida et al. [7] and Merkling et al. [8] are not sufficient to capture the dynamics of hydration in a bulk liquid and in particular the exchange with the molecules of the bulk. D'Angelo et al. [9] carried out a K-edge EXAFS study of bromide ions in aqueous solutions and combined them with classical molecular dynamics (CMD) simulations. They obtained a Br^-–O RdF, which they used with the integral form of the EXAFS equation to simulate an EXAFS spectrum in good agreement with the experiment. The integral form of the EXAFS

* Corresponding author. Tel.: +41 21 693 0457x0447; fax: +41 21 693 0422.
E-mail address: Majed.Chergui@epfl.ch (M. Chergui).

0301-0104/$ - see front matter © 2010 Elsevier B.V. All rights reserved.
doi:10.1016/j.chemphys.2010.03.023

equation [10], rather than the well-known discrete form [11], appears to be ideal for simulating EXAFS signals of disordered systems. While in D'Angelo et al.'s work the detailed orientation of water molecules around the bromide could not be retrieved because the H-atoms were neglected, their approach provided an oxygen coordination number (6.9) and first shell distance (3.34 Å) within the range of previous studies [5], consisting primarily of X-ray scattering measurements. The same approach was used by Wallen et al. [12] who extended the range of temperatures into the supercritical regime of water.

Recently, the valence level electronic structure of liquid water and of aqueous solutions of halide salts were studied by Winter and co-workers using photoelectron spectroscopy [13]. They found no effect by the halide salts on the binding energies of water, suggesting that perturbation by the salt ions is minimal. A different conclusion was reached by Cappa et al. [14] who carried out an oxygen K-edge absorption study of aqueous sodium halide solutions, finding that the electronic structure of adjacent molecules is significantly perturbed by the ions. This manifests itself by the appearance of an intensity increase of the pre-edge and main-edge absorptions. These results were interpreted by density functional theory (DFT) molecular dynamics (MD) of clusters of water around the ion, as arising from a strong direct perturbation of the unoccupied molecular orbitals of water by the anions, which does not require significant distortion of the hydrogen bond network beyond the first solvation shell.

From the above, it appears that the interpretation of experimental data, be it structural or electronic, heavily relies on computational simulations [2,5,8,9,14,15]. In the case of iodide, various force field-based computational MC or MD studies have been reported [3,16–18]. Structural data obtained from these simulations include an I^-–O RdF first peak in the range of 3.55–3.78 Å within the experimentally determined range of values [5], and an I^-–H first peak in the range of 2.55–2.93 Å. The first and second RdF peaks show incomplete separation, suggesting a diffuse solvation shell. The calculated coordination number varied from 7.3 to 9.7 (again in the range of experimentally determined values [5]) for oxygen and 6–6.6 for hydrogen atoms. The dynamical behaviour of the solvation shell is reflected by the residence time of water molecules in the first shell that ranges from 7.7 to 13.8 ps, depending on parameters of the force field. Recently, Heuft and Meijer [19] reported on a DFT-based MD simulation of a box of 64 water molecules and one I^- ion. They found a rather unstructured solvation shell, which they explained by the fact that the iodide–water hydrogen bonding is weaker than the water–water hydrogen bond. They also concluded that iodide has no effect on the dipole moment of the surrounding water molecules, which would agree with the valence band photoemission results of Winter et al. [20] In addition, the water molecules were found to bind to the ion for relatively short times of the order of 8–10 ps. Finally, their RdF's looked quite different to those derived by classical or hybrid Quantum Mechanics Molecular Mechanics (QM/MM) methods [3,18]. Very recently, Wick and Xantheas [21] carried out classical MD simulations with polarisable potentials of the aqueous solvation structure of chloride and iodide in the bulk and at interfaces, identifying an anisotropy of the solvation shell. A number of classical [17,22] and quantum simulation [23] studies had suggested the existence of a solvation shell anisotropy around halides, even in the presence of nonpolarizable anions [24].

It appears that most quantum simulations have been carried out on cluster models of water molecules around the halide [8,14,19], and that in general, few simulations (classical, hybrid QM/MM or quantum) have been checked against experimental observables. The approach by Filipponi and co-workers [9,10] based on the integral form of the EXAFS equation seems a simple and rather straightforward way of bench-marking the computational simulations against experimental data. It would identify which of the classical, hybrid or quantum simulations give the best radial distribution function, and in particular the first shell distance. As already mentioned, D'Angelo et al. [9] showed that CMD give a good description of the EXAFS spectra. However, given the extensive use of DFT methods for the description of water structure and dynamics [8,14,19,25], it is important to establish to what extent these quantum methods could provide a more realistic description of the shell structure around halides. Here, we perform classical, hybrid (QM/MM) and density functional theory (DFT) based MD simulations of aqueous solutions of iodide, which we use to simulate the EXAFS spectrum at the L_3-edge that we compare to the experimental spectrum, which we recorded.

The present work stems from our interest in the study of electronic solvation dynamics. The latter represents the reorganization of the solvent shell upon an electronic structure change of the solute. Given its importance in chemistry and biology, it represents one of the most studied processes in chemical physics, mainly using molecular dyes as solutes [26]. We previously proposed [27] an alternative approach based on atomic ions as solutes, whose electronic structure is modified by a short laser pulse that abstracts the electron, while probing is done by ultrafast X-ray absorption spectroscopy. We recently demonstrated the feasibility of such experiments by recording the transient XAS spectrum of an aqueous iodide solution at the $L_{1,3}$ edges of iodine 50 ps after laser excitation [28,29], while a similar study was later reported on bromide ions [30]. Clear signatures of both electronic (resulting from the electron abstraction) and solvent shell structure changes could be read off the spectra. However, a quantitative analysis of the solvent shell reorganization relies on a clear description of the solvation shell structure around I^- prior to laser excitation, which is the object of this contribution.

2. Experimental methods

A 500 mM iodide aqueous solution was prepared by dissolving sodium iodide (99.9% purity) in distilled water. The sample is circulated in a free flowing liquid jet of 200 μm thickness. X-ray absorption spectra at the iodine L_3-edge were recorded in transmission mode at the micro-XAS beamline of the Swiss Light Source (Villigen, Switzerland), using the third harmonic of the undulator. An Si(1 1 1) double crystal monochromator was used, giving an energy resolution of 0.8 eV in the measured energy range. Two ionization chambers filled with He at 1 bar were utilized to measure the incoming and the transmitted beam intensity through the sample. The synchrotron was operated at 350 mA. The incident fluxes at the sample position are typically 5.5×10^{11} ph/s at the L_3-edge (4.56 keV).

3. Computational methods

3.1. Classical MD

All classical MD simulations used for the equilibration of the QM and QM/MM set-ups were performed in the isothermal–isobaric ensemble (NPT) using the AMBER 7 package with the nonpolarizable parm99 force field. The system is made of one I^- ion solvated in 1192 TIP3P water molecules in a cubic box of (33.6 Å) [3], using periodic boundary conditions. The system was equilibrated for 10 ns with a time-step of 1 fs and was maintained at 300 K and 1 atm by thermo- and barostats of the Berendsen type. Electrostatic interactions were treated using the particle mesh Ewald scheme. The last 5 ns of the MD run was used to compute the structural properties of iodide solvation shells at a classical level.

3.2. Full-DFT setup and first principle MD simulations

In the full-DFT setup, aqueous iodide was modelled using a periodically replicated cubic simulation supercell of side 18.15 Å, containing one iodide ion and 183 water molecules. The cell size and the number of water molecules were determined by imposing that the iodine–water system yields a total pressure equal to a sample of liquid water at room temperature and standard pressure (1 atm). To this end, a classical MD trajectory of 10 ns at 300 K and 1 atm was computed to set up the initial configuration for the DFT-based MD simulations.

The system composed of a solvated iodide ion and the water molecules was treated within periodic boundary conditions and the Kohn–Sham orbitals were expanded in plane-waves at the Γ point of the Brillouin zone up to a kinetic energy cutoff of 100 Ry.

All DFT calculations were performed using Troullier–Martins-type pseudopotentials for the core electrons. Integration of the nonlocal parts of the pseudopotential was performed using the Kleinman–Bylander scheme. The exchange and correlation potential was described at the BLYP level of theory. A short preparation run of ~2 ps was performed starting from the classically equilibrated geometry. This was followed by a production run of 5.5 ps that was used to sample the trajectory for the analysis of the iodide solvation geometries.

All DFT-based MD simulations were performed using the Born–Oppenheimer scheme with a time-step of 15 a.u. During the preparation run which follows the classical equilibration, the temperature was controlled through a Nosé–Hoover thermostat. The production runs were performed in the microcanonical ensemble at constant energy using the software package CPMD [31].

3.3. QM/MM setup and QM/MM MD simulations

The QM/MM setup consists of a single iodide ion described at a DFT level of theory solvated in a classical bath of 1192 TIP3P water molecules in a box of (33.6 Å) [3]. The force field parameters used for the water molecules are those employed in the classical MD simulations. The quantum part of the system was confined in a cubic box with 12 Å edge, but classical water molecules could enter the QM box. The inherent periodicity in the plane-wave calculations was circumvented by solving the Poisson equation for non-periodic boundary conditions, while periodic boundary conditions were retained for the classical solvent box. All other simulation conditions for the QM part (the I^- ion) and MD parameters were kept identical to the ones used in the full-DFT MD simulations. The steric interaction between the QM and the MM part were modelled by a Lennard–Jones potential as described by the parm99 force field, while the electrostatic interactions with the neighbouring MM atoms were described by a fully Hamiltonian hierarchical coupling scheme [32] as implemented in the CPMD code.

The simulation protocol follows closely the one used for the full-DFT MD calculations. The only difference lies in the quality of the sampling (trajectory length) since the QM/MM approach is computationally less demanding and allows therefore longer simulation times. The QM/MM radial distribution functions were computed from a single trajectory of 15 ps.

4. Simulations of the EXAFS spectra

For the hydration shell of halogen anions, particularly those with large radii, the main contribution to the EXAFS signal is associated with the single scattering events that reflect a two-body interaction. Rather than using the usual discrete form of the EXAFS equation [11], the signal is modelled as a function of the radial distribution function $g(r)$ as [10]:

$$\chi(k) = \int_0^\infty 4\pi\rho_O r^2 g_{I^-O}(r) A_O(k,r)\sin(2kr + \phi_O(k,r))dr + \int_0^\infty 4\pi\rho_H r^2 g_{I^-H}(r) A_H(k,r)\sin(2kr + \phi_H(k,r))dr \quad (1)$$

where $A(k,r)$ and $\Phi(k,r)$ are the amplitude and phase functions. An average hydration shell structure, described by radial pair distribution functions, can be extracted from the analysis of the EXAFS signal using Eq. (1). Theoretical EXAFS signal at the iodine L_3-edge associated with the oxygen and hydrogen atoms of the first shell water molecules, are calculated from Eq. (1) using the GNXAS program [10,33]. The phase shifts $\Phi(k,r)$ are calculated from a snapshot of atomic coordination given by the MD simulations. A Hedin–Lundqvist (HL) plasmon-pole was used for the phase shift calculation with muffin-tin radii for iodide, oxygen and hydrogen of 2.28, 0.9, and 0.21 Å, respectively. Inelastic losses of the photoelectron are accounted for by complex potentials where the imaginary part includes core–hole width of 3.08 eV for the $2p_{3/2}$ hole [34]. The $\chi(k)$ signal is mainly sensitive to a limited distance from the absorber due to the finite photoelectron mean-free path, this effect together with the spectral damping due to monochromator resolution are included in the scattering amplitude $A(k,r)$. Reduction amplitude S_0^2, accounting for a uniform reduction of the signal associated with many-body effects, is set to 1. The total $\chi(k)$ contribution which is the sum of the two-body signals from oxygen and hydrogen atoms were shifted in energy space to fit the experiment. The agreement between the theory and the experiment is then evaluated by sum of squared error (SSE) value expressed in Eq. (2).

$$\mathrm{SSE} = \sum_{i=1}^{N} \left(\chi_i^{\mathrm{exp}} - \chi_i^{\mathrm{theo}}\right)^2 \quad (2)$$

where χ_i^{exp} and χ_i^{theo} are experimental and theoretical EXAFS signal for each data point i.

5. Results and discussion

Fig. 1 shows the L_3–edge XAS spectrum of aqueous iodide at room temperature. Fig. 2 shows the I^-–O and I^-–H $g(r)$'s from the classical, the QM/MM and the DFT MD simulations. These $g(r)$'s are in agreement with those of the literature both for the classical [3,18,21] and the DFT simulations [19]. The DFT $g(r)$'s point to a smaller density of water molecules in the first shell than the classical or QM/MM simulations. Finally, the classical and DFT simulations point to a more pronounced solvation shell structure than the QM/MM ones. The dotted trace in Fig. 3 is the L_3-edge

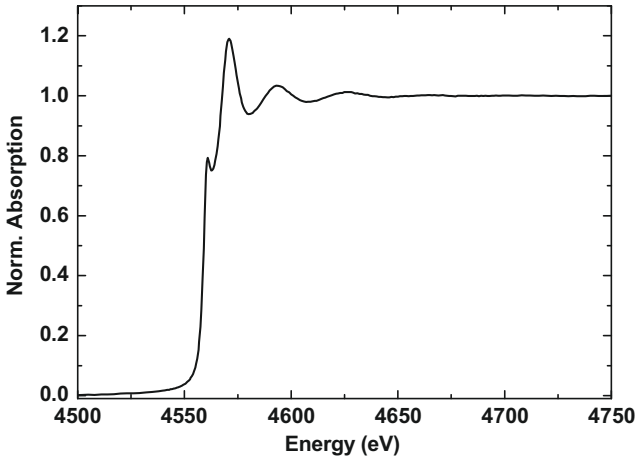

Fig. 1. Aqueous iodide L_3-edge absorption spectrum.

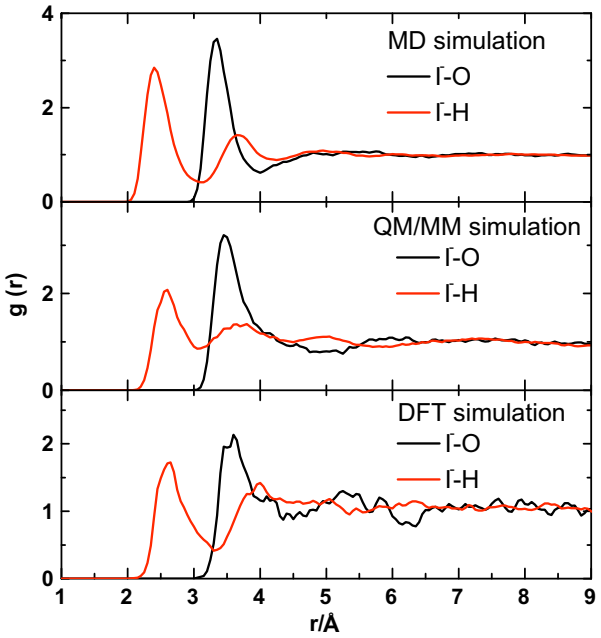

Fig. 2. Radial distribution function around iodide of the oxygen (black) and hydrogen (red) atoms of water molecules to iodide from classical MD, QM/MM and DFT simulations.

EXAFS spectrum extracted from the raw data with Pyspline [35], a program for EXAFS data reduction. The background was modelled by three segmented cubic functions.

Fig. 3 compares the experimental and theoretical $\chi(k)$ spectra, calculated from Eq. (1) using the $g(r)$'s of Fig. 2. The structural parameters derived from the classical, QM/MM and DFT simulations have been kept fixed in the EXAFS analysis. In this way the first hydration shell structure obtained from the simulations can be directly compared with experimental data and the validity of the theoretical framework used in the simulations can be assessed. The upper panels of Fig. 3 show the separate I–H and I–O first shell contributions as derived from their respective $g(r)$'s (Fig. 2). The sum of these two contributions (total) is overlaid onto the EXAFS experimental signal, and the resulting residuals are also shown. It is clear that the classical and QM/MM-based $g(r)$'s deliver a better agreement with the experimental data than the DFT simulations. The classical MD is quite satisfactory but shows deviations in the high k region, whereas the QM/MM-based $g(r)$ provides a better agreement, and therefore represents a more accurate description of the solvent shell structure. The introduction of the H-atom contributions in the simulations of EXAFS signals is a non-trivial problem and is still a subject of debate [36], as it is not clear where the charge is located. While it improves the fit, it is clear from Fig. 3 that it is not needed, and the classical and QM/MM simulations are still preferable to the DFT ones.

If we consider the good description of the EXAFS signal obtained from the present hybrid QM/MM simulations and the pure classical simulations of D'Angelo et al. on aqueous Br^- [9], it appears that the main reason for the poorer agreement with the DFT-based simulations lies in the quality of the water–water intermolecular interactions and the fact that these are comparable to the solute–water interaction. Indeed for solutes with an ordered solvent shell, such as aqueous Co^{2+} which forms a $Co(H_2O)_6$ complex, DFT MD did generate a structure that satisfactorily reproduces the EXAFS spectrum [37]. Previous studies have shown that the outcome of DFT-based MD simulations of liquid water is very sensitive to the particular choice of the functional [38] and basis set [39]. Water

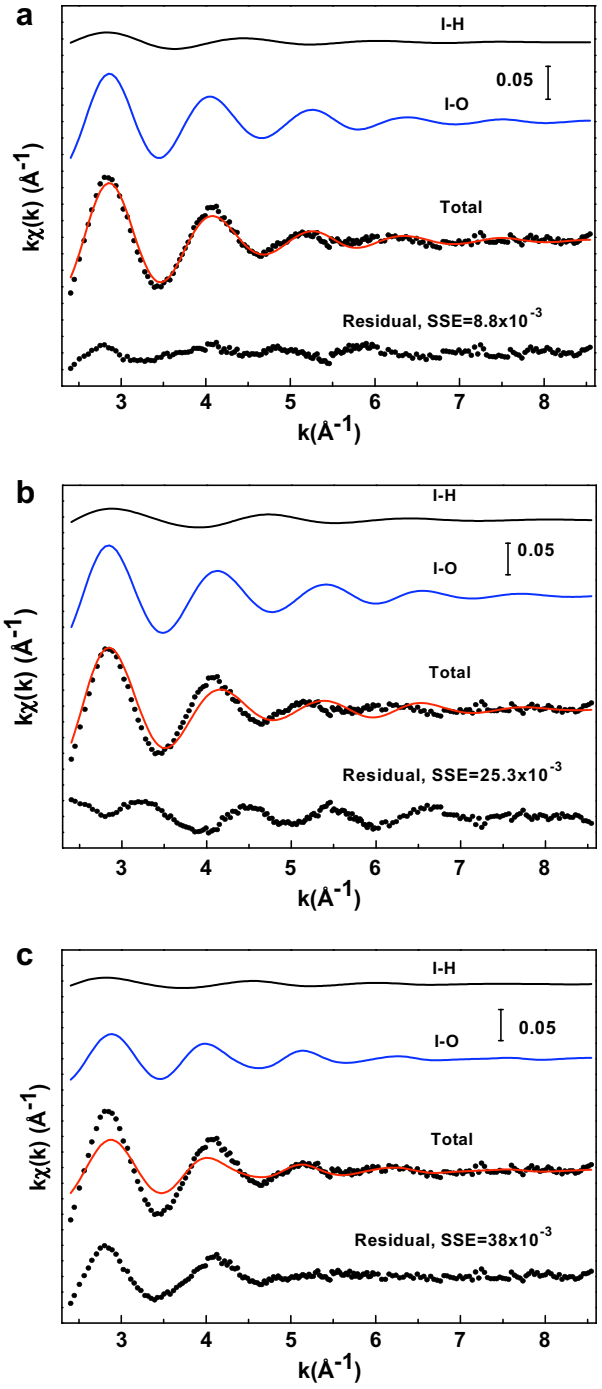

Fig. 3. Theoretical EXAFS calculations from the simulated QM/MM (a), CMD (b) and DFT (c) structures. The black and blue curves are EXAFS signal associated with I–H and I–O scattering, respectively. The red curves are total EXAFS signals. The upper dotted black curves are the experiment, the lower ones are residual between the theory and the experiment. The quality of the calculations (SSE) is given in the graphs.

computed at DFT level within the generalized gradient approximation (GGA) for the exchange–correlation functional is generally over structured and diffuses one order of magnitude more slowly than experimentally determined. Hybrid functionals improve the predictions slightly [40], and the reason for such discrepancies was the subject of a recent theoretical study [41]. It is generally believed that the structure of liquid water stems from the competition between H-bond and van der Waals (vdW) interactions [42].

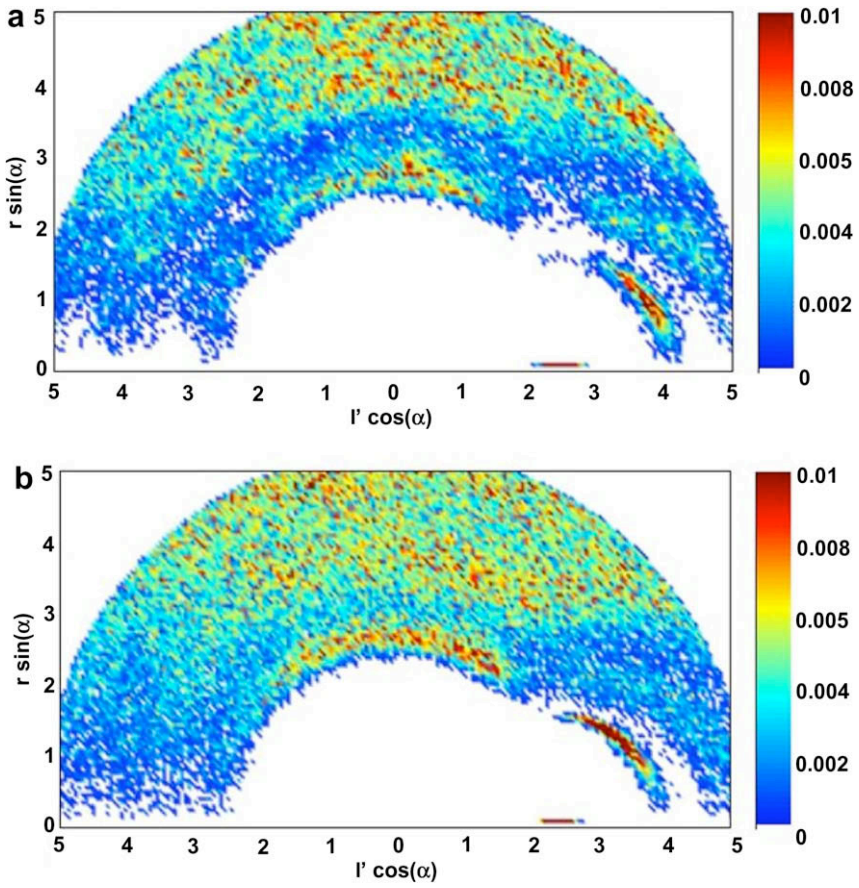

Fig. 4. Radial-angular distribution function (RADF) of iodide anions with the water hydrogen atoms obtained from the DFT (a) and the QM/MM (b) simulations. The reference is the direction between the iodide and the closest H-atom (that may change from one frame to the other, but not so frequently). We define the angle α between this reference axis and the anion-hydrogen vector (a value of $\alpha = 0$ defines the direction towards the closest H-atom).

Even though DFT-GGA has been successful in describing a wide variety of strongly interacting systems, it has not found equal success in describing weak interactions.

Of special importance here is the determination of anisotropy of the solvation shell. In Ref. [21], using classical molecular dynamics simulations with polarisable potentials the authors identified an anisotropy in the radial-angular distribution function (RADF) of water around iodide. They used the same definition of the distance as in the radial distribution function, but defined the angle between the anion-hydrogen vector and the induced dipole vector of the anion. The solvation shell was clearly anisotropic with a very low probability of finding anions near the region in which the induced dipoles are pointing away, and with a high probability of finding hydrogen atoms on the other side. Given the weakness of the anion induced dipole, one may ask if this anisotropy is real. Therefore, in order to address this point, here we adopt a different approach. Instead of using the direction of the dipole on the ion, we take as reference the direction between the iodide and the closest H-atom (that may change from one frame to the other, but not so frequently) and for all anion-hydrogen vectors in the sample we compute the corresponding angles α_i formed with the reference axis, and their length, r_i. The index i runs over all H-atoms and a value of $\alpha = 0$ defines the direction towards the closest H-atom. The result is shown in Fig. 4, where we plot the RADF sampled along our trajectories (which corresponds to the probability of all $\{\alpha_i, r_i\}$ pairs) as a function of $r\cos(\alpha)$ and $r\sin(\alpha)$. For the sake of comparison, we present the result for both the DFT and QM/MM MD simulations. Interestingly, we find a rather structured distribution of water H-atoms in the first solvation shell of I^-. Along the abscissae at a distance of about 2.5 Å ($\alpha = 0$ is the distribution of the closest H-atom, which has a standard deviation of about 0.3 Å in both full DFT and QM/MM simulations. In the same direction, at small angular deviations from the reference axis, the distributions of the second and third closest H-atoms are also well resolved. Overall, the agreement between the two simulation set-ups is good, even though a slightly more structured RADF is observed in the full DFT calculation in agreement with what was observed for the radial distribution functions. The occurrence of an anisotropy of the solvation shell is of importance for the study of the ejection of the electron upon ultraviolet excitation of the so-called charge-transfer-to-solvent bands [43]. A contact pair formed of iodine and the electron has been postulated as an intermediate, with the electron cloud filling the voids of the solvation shell in an anisotropic fashion [44].

6. Conclusions

In conclusion, we have performed classical, hybrid QM/MM and full quantum (DFT) molecular dynamics simulations of iodide in water, which we have calibrated against experimental EXAFS spectra at the L_3-edge. It appears that for aqueous halides QM/MM and nonpolarizable classical simulations deliver a better description of the solvation shell. In particular, QM/MM offers the potential of a more precise description of the quantum part due to the solute–solvent interaction, while allowing simulations over several picoseconds. We discussed the origin of the discrepancies of DFT MD, but we stress that they are peculiar to the case of weak

solute–solvent interactions, leading to disordered solvation shells. We also show that the solvation shell around iodide is anisotropic, a feature that is of importance when discussing the solvent shell rearrangements upon light excitation of the system [28].

Acknowledgments

We thank the Swiss NSF for support via contracts 200021-107956, 200021-105239/1 and 200020-116533 and the Sekretariat für Bildung und Forschung via contract COST D 35 060016. We also thank the Pleiades Cluster for High Performance Computing (HPC) resource.

References

[1] K. Ando, J.T. Hynes, J. Phys. Chem. B 101 (49) (1997) 10464.
[2] D. Laage, J.T. Hynes, Proc. Natl. Acad. Sci. USA 104 (27) (2007) 11167.
[3] S. Koneshan, J.C. Rasaiah, R.M. Lynden-Bell, S.H. Lee, J. Phys. Chem. B 102 (21) (1998) 4193.
[4] E. Gouaux, R. MacKinnon, Science 310 (5753) (2005) 1461.
[5] H. Ohtaki, T. Radnai, Chem. Rev. 93 (3) (1993) 1157.
[6] R.M. Lawrence, R.F. Kruh, J. Chem. Phys. 47 (11) (1967) 4758;
A.K. Soper, J. Phys.-Condens. Matter 9 (13) (1997) 2717.
[7] H. Tanida, K. Kato, I. Watanabe, Bull. Chem. Soc. Jpn. 76 (9) (2003) 1735.
[8] P.J. Merkling, R. Ayala, J.M. Martinez, R.R. Pappalardo, E.S. Marcos, J. Chem. Phys. 119 (13) (2003) 6647.
[9] P. D'Angelo, A. Dinola, A. Filipponi, N.V. Pavel, D. Roccatano, J. Chem. Phys. 100 (2) (1994) 985.
[10] A. Filipponi, J. Phys.-Condens. Matter 6 (41) (1994) 8415.
[11] J.J. Rehr, R.C. Albers, Rev. Mod. Phys. 72 (3) (2000) 621.
[12] S.L. Wallen, B.J. Palmer, D.M. Pfund, J.L. Fulton, M. Newville, Y.J. Ma, E.A. Stern, J. Phys. Chem. A 101 (50) (1997) 9632.
[13] R. Weber, B. Winter, P.M. Schmidt, W. Widdra, I.V. Hertel, M. Dittmar, M. Faubel, J. Phys. Chem. B 108 (15) (2004) 4729.
[14] C.D. Cappa, J.D. Smith, K.R. Wilson, B.M. Messer, M.K. Gilles, R.C. Cohen, R.J. Saykally, J. Phys. Chem. B 109 (15) (2005) 7046.
[15] B. Winter, M. Faubel, Chem. Rev. 106 (4) (2006) 1176.
[16] E. Brodskaya, A.P. Lyubartsev, A. Laaksonen, J. Chem. Phys. 116 (18) (2002) 7879;
A. Ignaczak, J.A.N.F. Gomes, M.N.D.S. Cordeiro, Electrochim. Acta 45 (4–5) (1999) 659;
P. Jungwirth, D.J. Tobias, Chem. Rev. 106 (4) (2006) 1259.
[17] L.X. Dang, B.C. Garrett, J. Chem. Phys. 99 (4) (1993) 2972.
[18] B. Hribar, N.T. Southall, V. Vlachy, K.A. Dill, J. Am. Chem. Soc. 124 (41) (2002) 12302.
[19] J.M. Heuft, E.J. Meijer, J. Chem. Phys. 123 (2005). 9.
[20] B. Winter, R. Weber, W. Widdra, M. Dittmar, M. Faubel, I.V. Hertel, J. Phys. Chem. A 108 (14) (2004) 2625.
[21] C.A. Wick, S.S. Xantheas, J. Phys. Chem. B 113 (13) (2009) 4141.
[22] M.A. Carignano, G. Karlstrom, P. Linse, J. Phys. Chem. B 101 (7) (1997) 1142.
[23] H.A. Stern, G.A. Kaminski, J.L. Banks, R.H. Zhou, B.J. Berne, R.A. Friesner, J. Phys. Chem. B 103 (22) (1999) 4730;
S. Raugei, M.L. Klein, J. Chem. Phys. 116 (1) (2002) 196.
[24] S. Rajamani, T. Ghosh, S. Garde, J. Chem. Phys. 120 (9) (2004) 4457.
[25] B. Winter, E.F. Aziz, U. Hergenhahn, M. Faubel, I.V. Hertel, J. Chem. Phys. 126 (2007). 12;
B. Winter, E.F. Aziz, N. Ottosson, M. Faubel, N. Kosugi, I.V. Hertel, J. Am. Chem. Soc. 130 (22) (2008) 7130.
[26] O. Kühn, L. Wöste, Analysis and Control of Ultrafast Photoinduced Reactions, Springer, Berlin, New York, 2007.
[27] C. Bressler, M. Saes, M. Chergui, D. Grolimund, R. Abela, P. Pattison, J. Chem. Phys. 116 (7) (2002) 2955.
[28] V.T. Pham, W. Gawelda, Y. Zaushitsyn, M. Kaiser, D. Grolimund, S.L. Johnson, R. Abela, C. Bressler, M. Chergui, J. Am. Chem. Soc. 129 (6) (2007) 1530.
[29] C. Bressler, R. Abela, M. Chergui, Z. Kristallogr. 223 (4–5) (2008) 307.
[30] C.G. Elles, I.A. Shkrob, R.A. Crowell, D.A. Arms, E.C. Landahl, J. Chem. Phys. 128 (2008). 6.
[31] C.I. Corp, 1990–2004.
[32] A. Laio, J. VandeVondele, U. Rothlisberger, J. Chem. Phys. 116 (16) (2002) 6941.
[33] <http://gnxas.unicam.it/XASLABwww/pag_gnxas.html>.
[34] M.O. Krause, J. Phys. Chem. Ref. Data 8 (2) (1979) 307.
[35] A. Tenderholt, B. Hedman, K.O. Hodgson, in: Presented at The 13th International Conference on X-ray Absorption Fine Structure (XAFS13), Stanford, California, 2006 (unpublished).
[36] U. Bergmann, A. Di Cicco, P. Wernet, E. Principi, P. Glatzel, A. Nilsson, J. Chem. Phys. 127 (17) (2007) 174504;
U. Bergmann, A. Di Cicco, P. Wernet, E. Principi, P. Glatzel, A. Nilsson, J. Chem. Phys. 128 (8) (2008) 089902.
[37] R. Spezia, M. Duvail, P. Vitorge, T. Cartailler, J. Tortajada, G. Chillemi, P. D'Angelo, M.P. Gaigeot, J. Phys. Chem. A 110 (48) (2006) 13081.
[38] J. VandeVondele, F. Mohamed, M. Krack, J. Hutter, M. Sprik, M. Parrinello, J. Chem. Phys. 122 (1) (2005) 014515.
[39] H.S. Lee, M.E. Tuckerman, J. Chem. Phys. 125 (15) (2006) 154507.
[40] T. Todorova, A.P. Seitsonen, J. Hutter, I.F.W. Kuo, C.J. Mundy, J. Phys. Chem. B 110 (8) (2006) 3685.
[41] I.C. Lin, A.P. Seitsonen, M.D. Coutinho-Neto, I. Tavernelli, U. Rothlisberger, J. Phys. Chem. B 113 (4) (2009) 1127.
[42] C.H. Cho, S. Singh, G.W. Robinson, J. Chem. Phys. 107 (19) (1997) 7979.
[43] X.Y. Chen, S.E. Bradforth, Annu. Rev. Phys. Chem. 59 (2008) 203.
[44] S.E. Bradforth, P. Jungwirth, J. Phys. Chem. A 106 (7) (2002) 1286.